

Reproduced by
AIR DOCUMENTS DIVISION



HEADQUARTERS AIR MATERIEL COMMAND
WRIGHT FIELD, DAYTON, OHIO

The
U.S. GOVERNMENT

IS ABSOLVED

FROM ANY LITIGATION WHICH MAY
ENSUE FROM THE CONTRACTORS IN-
FRINGING ON THE FOREIGN PATENT
RIGHTS WHICH MAY BE INVOLVED.

WRIGHT FIELD, DAYTON, OHIO

REEL - C

4 8 2

A.T.I.

1 3 8 0 0

UNCLASSIFIED

95
981

MEASUREMENTS ON NOISE FROM REFLEX OSCILLATORS

REPORT

872

DL

<input type="checkbox"/> Chief	<input type="checkbox"/> Admin.	<input type="checkbox"/> Initial & Data
<input type="checkbox"/> Asst. Chief	<input type="checkbox"/> Insp.	<input type="checkbox"/> Return
<input type="checkbox"/> Ch. of Eng.	<input type="checkbox"/> Rec.	<input type="checkbox"/> Your File
<input type="checkbox"/> Sr. Supt.	<input type="checkbox"/> Nav.	<input type="checkbox"/> Rec. Action
<input type="checkbox"/> Executive	<input type="checkbox"/> A. D.	<input type="checkbox"/> Info. Only
<input type="checkbox"/> Asst. Exec.	<input type="checkbox"/> S. H.	<input type="checkbox"/> Mail Unit

RADIATION LABORATORY
MASSACHUSETTS INSTITUTE OF TECHNOLOGY
CAMBRIDGE MASSACHUSETTS

1. RZA
2. HZR
3. AOL
4. BTO
T. E.

<input type="checkbox"/> Ch. Elect. Subdiv.	<input checked="" type="checkbox"/> Radar Lab.
<input type="checkbox"/> Asst. Ch. Elect. Subdiv.	<input type="checkbox"/> Proc. Inf. Sec.
<input type="checkbox"/> Tech. Asst.	<input type="checkbox"/> Syst. Eng. Lab.
<input type="checkbox"/> Admin. Asst.	<input type="checkbox"/> Eng. Serv. Lab.
<input type="checkbox"/> Spec. Pers.	<input type="checkbox"/> Fkt. Install.
<input type="checkbox"/> C & N Lab.	<input type="checkbox"/> Files
<input type="checkbox"/> Spec. Prod. Lab.	<input type="checkbox"/> Patent Agency

1/9/46

108



ATI No. 13800

NRCC
Div. 14
Ottawa-262

Radiation Laboratory

Report 872

December 21, 1945

MEASUREMENTS ON NOISE FROM REFLEX OSCILLATORS

Abstract

A program of measurements on noise output of reflex local oscillators, particularly the 722A/B and 2H33, was undertaken to try to determine the importance of this factor in receiver design. Considering the two noise sidebands each 2.5 mc/sec wide and located 30 Mc/sec away from the main output, we found noise powers ranging from 2.2 to 9.8×10^{-12} watts coming out of 722A/B's loaded for optimum output. Asymmetrical behavior of the noise with electronic tuning was investigated and found to require the new theory presented in the companion report number 873 by J. K. Kaipp. Some measurements of the individual noise sidebands and of the noise output as a function of load were found to be in satisfactory agreement with theory.

J. B. H. Kuper
M. O. Walts

Approved by:

A. E. Whitford
Leader, Group 63

A. H. Hill
Head, Division 6

Title page
16 numbered pages

MEASUREMENTS ON NOISE FROM REFLEX OSCILLATORS

Introduction

Although it has been known for about three years¹ that local oscillators can contribute appreciable noise in microwave receivers, the experimental data have been rather scanty. In view of the fact that the trend to higher radio frequencies and the steady improvement in converters both tend to magnify the importance of this source of noise, it was decided to undertake a measurement program covering particularly the reflex triode variation tubes used at X and L bands. The recent introduction of balanced mixers which eliminate this noise has greatly reduced the practical importance of this work but nevertheless it may be of interest for the light it affords on the behavior of reflex oscillators. It was intended to study the noise output of a group of tubes under reproducible conditions, to attempt to determine the effects of different tube designs, as well as to obtain numerical information for the use of the circuit designer. With this in mind measurements with i-f's of 30, 60 and 90 mc were made first on a group of 723A/2 tubes and later on some assorted X-band oscillators.

While the measurements were in progress, a paper by Pierce² appeared and we devoted considerable effort to attempts to verify his calculations. Our conclusion was that his theory appeared to predict correctly the effects of changes in tube design or load conditions on noise at the center of the electrical tuning range, but that it was incapable of accounting for the large variations we found with electrical tuning. At this stage Dr. Knipp started on a more complete theory set forth in a companion paper³ which seems capable of accounting fully for the observations.

Pierce's theory considered three mechanisms by which noise could be introduced to the i-f: 1) the "high frequency noise", thought of as shot (and interception) noise in the beam coupled out through the cavity, 2) "low frequency noise" due to amplitude modulation of the oscillator by noise components in the beam at i-f, and 3) frequency modulation due to fluctuations (near i-f) in phase of the returning electrons. Experimentally it seems that with adequate bypassing⁴ of the leads to the oscillator tube mechanisms 2) and 3) are relatively unimportant.

Aside from differences in approach, Knipp's theory is an extension of Pierce's consideration of the high frequency noise, 1) in which he takes account a) of the coherence between the first and second passage of the electrons through the gap, and b) of noise due to mixing of various components in the beam with harmonics of the oscillator current. The coherence n) introduces a strong variation with electrical tuning, in accord with our results. In most of our experiments noise due to the two sidebands, corresponding to "signal" and "image" in ordinary superheterodyne reception, was measured without any attempt of selection. In Knipp's theory, on the other hand, the two bands are calculated separately and then summed for comparison with experiment. The contributions are in general not equal.

1. Sherwood and Ginston, Sperry Gyroscope Co. Report 5520-107
Rack, Bell Telephone Labs Report RM-42-130-55
Rosen, Standard Telephone and Cable Co. Report 2266 (0) - (WRS11)
Rees, Radiation Lab Report 51-22
2. Pierce, Bell Telephone Labs Report RM-44-140-4
3. Knipp, Radiation Lab Report 573
4. The importance of good bypassing can scarcely be overestimated. Lack of it could introduce astonishing amounts of noise in some circumstances.

Method of Measurement

In most of the prior work on oscillator noise the measurements were made using a resonant cavity filter to remove the noise sidebands from the oscillator output. In the present work this scheme was avoided as we desired to present a non-reactive load to both the mixer and the oscillator under test. Instead the "temperature" of the crystal was measured for various conditions using the set-up shown in Fig. 1, in which the output due to crystal noise was compared with the noise from a resistor of equivalent i-f impedance.

We have the familiar relation for noise figure (in times) of a receiver

$$F = \frac{T_o + F_{IF} - 1}{G_o}$$

where F is the overall noise figure, T_o and G_o the "temperature" and conversion gain of the crystal, and F_{IF} the noise figure of the i-f amplifier. If additional noise power from the local oscillator P_{NL} (in watts for the bandwidth B) is fed to the input we have

$$F' = \frac{P_{NL}}{kTB} + \frac{T_o + F_{IF} - 1}{G_o} \\ = \frac{T_o' + F_{IF} - 1}{G_o}$$

where $T_o' = T_o + \frac{G_o P_{NL}}{kTB}$ is an apparent crystal "temperature" including the effects of oscillator noise.

Let P_N be the local oscillator power fed to the crystal and P/P the "noise/signal" ratio (noise output power in a band B over oscillator output) for the oscillator. We have $P_{NL} = (P_N/P) P_X$. If we measure T_o' under standard conditions, say 0.5 ma crystal current, P_X will vary roughly as $1/G_o$, and to a first approximation $T_o' - T_o$ is proportional to the local oscillator noise ratio P_N/P and not dependent on the properties of the crystal used.

Throughout the X-band measurements we used one crystal which had $G_o = -7$ db and $T_o = 1.2$, and a coupling was always adjusted to give a rectified current of 0.5 ma. The crystal parameters were frequently checked and remained quite constant.

As indicated in Fig. 1, the measuring set consisted of three preamplifiers tuned to 30, 60 and 90 mc, and a main amplifier about 2.5 mc wide tuned to 30 mc which incorporated an i-f attenuator and power output meter. In the case of the 60 and 90 mc preamplifiers a second conversion to 30 mc was employed.

Coupling between the mixer and preamplifier was by a coaxial line transformer so arranged that shifting i-f involved only changing two cables, and did not affect the crystal properties. A noise diode was mounted on the mixer so that F_{IF} could be measured in the three cases.

The tube was mounted on a section $5/8" \times 1 1/4"$ (outside) waveguide with the antenna located centrally in the guide. A choke plunger in the end of the guide was

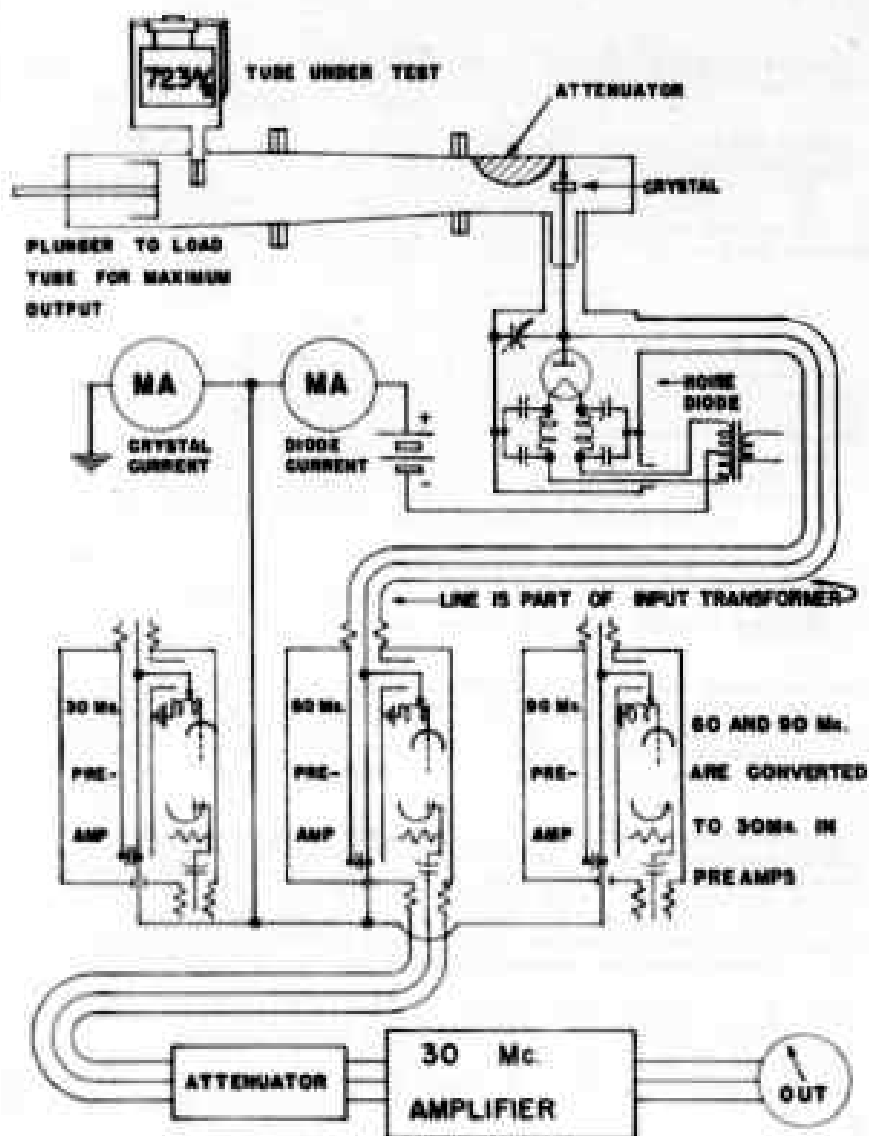


FIG. 1

adjusted for each tube to obtain maximum output. A taper was employed to reduce to $\frac{1}{8}$ x $\frac{1}{8}$ inch guide and a standard flap attenuator served to adjust crystal current. The crystal holder was of conventional design.

This plumbing was used for most of the measurements reported here and similar arrangements were employed at K-band. To permit separation of the noise side bands in one experiment it was modified by the introduction of a filter cavity on a T connection between the pad and the crystal to reject one component at will. In this case it would have been preferable to avoid changes in crystal gain and i-f impedance by additional padding between the crystal and the T but the local oscillator power was not sufficient to permit this.

Results

The first measurements were a series of controls to establish the validity of the scheme. In these the output power of the 7234/B was varied in some manner not likely to affect the noise output materially, say by changing the resonator voltage. The attenuation was readjusted to give the same crystal current, and P and T_0 were observed at the three i-f's. When T_0 for the center of the electrical tuning range in a given mode (which we have called the "head on" condition) is plotted against $1/P$ the result is a straight line for each i-f. This line if produced would intersect the ordinate axis at a constant value for T_0 , in agreement with the value 1.2 previously determined. A typical plot of this sort is shown as Fig. 2.

It was noticed at once that if the power output of the oscillator was varied by electrical tuning that the plots could no longer be produced back to the common intercept, as indicated by the dotted lines in Fig. 2. Also there was a strong dependence on the direction of electrical tuning, increasing frequency giving increased noise.

Definite asymmetry in noise output as a function of electrical tuning had been observed before (cf. curves in Beere's report) but was apparently ascribed to a peculiarity of the r-f properties of the mixer and more or less ignored. In our experiments no high Q elements were present and the asymmetry was so prominent it could not be passed over, partly because we had the tube tightly coupled to the wave guide.

For convenience we made our measurements generally in three conditions, tuned "head on" and detuned by variation of reflector voltage to the two half-power points (designated as " $\frac{1}{2}$ high" and " $\frac{1}{2}$ low"). It was soon found that the ratio of the noise outputs at the two half-power points, the "high/low ratio", varied from tube to tube and also depended on mode used and i-f for a given tube. In Table I we illustrate the data obtained on one 7234/B at three i-f's and for five reflector modes, together with the power output and electrical tuning range between half power points.

As might be expected the noise decreases rapidly when the i-f is raised. Indeed the decrease in noise is so marked that not much importance need be attached to the 90 mc data, as the experimental error must be considerable. It should be mentioned that at the half power points the coupling was doubled (to keep the crystal current constant) and therefore if noise output alone is of interest $T_0' - T_0$ for the half power points should be divided by 2.

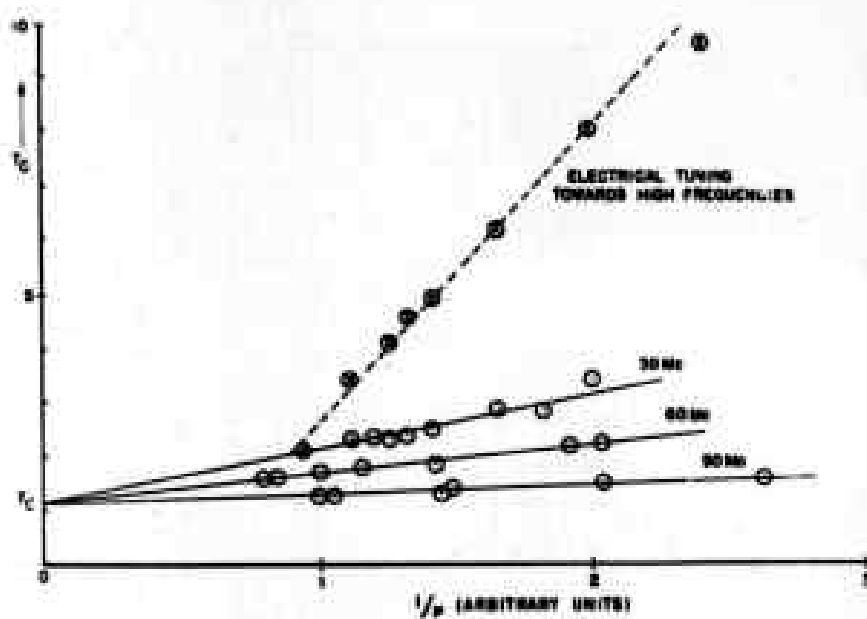


FIGURE 2

Table 1

Tube (pencil (7.5.))		Int. Voltage = 200		$T_2 = 1.4$		$T_2 = 1.5$ cm	
Deflection Scale	30 sec.	$T_2 = T_1$		60 sec.		Stagnation Pressure mm.	Deflection Scale
		$T_2 = T_1$		$T_2 = T_1$			
		Read on 1000 ft	1000 ft	Read on 1000 ft	1000 ft		
0.5 mm	100	100	100	100	100	100	100
1.0 mm	200	200	200	200	200	200	200
1.5 mm	300	300	300	300	300	300	300
2.0 mm	400	400	400	400	400	400	400
2.5 mm	500	500	500	500	500	500	500
3.0 mm	600	600	600	600	600	600	600
3.5 mm	700	700	700	700	700	700	700
4.0 mm	800	800	800	800	800	800	800
4.5 mm	900	900	900	900	900	900	900
5.0 mm	1000	1000	1000	1000	1000	1000	1000
5.5 mm	1100	1100	1100	1100	1100	1100	1100
6.0 mm	1200	1200	1200	1200	1200	1200	1200
6.5 mm	1300	1300	1300	1300	1300	1300	1300
7.0 mm	1400	1400	1400	1400	1400	1400	1400
7.5 mm	1500	1500	1500	1500	1500	1500	1500
8.0 mm	1600	1600	1600	1600	1600	1600	1600
8.5 mm	1700	1700	1700	1700	1700	1700	1700
9.0 mm	1800	1800	1800	1800	1800	1800	1800
9.5 mm	1900	1900	1900	1900	1900	1900	1900
10.0 mm	2000	2000	2000	2000	2000	2000	2000
10.5 mm	2100	2100	2100	2100	2100	2100	2100
11.0 mm	2200	2200	2200	2200	2200	2200	2200
11.5 mm	2300	2300	2300	2300	2300	2300	2300
12.0 mm	2400	2400	2400	2400	2400	2400	2400
12.5 mm	2500	2500	2500	2500	2500	2500	2500
13.0 mm	2600	2600	2600	2600	2600	2600	2600
13.5 mm	2700	2700	2700	2700	2700	2700	2700
14.0 mm	2800	2800	2800	2800	2800	2800	2800
14.5 mm	2900	2900	2900	2900	2900	2900	2900
15.0 mm	3000	3000	3000	3000	3000	3000	3000
15.5 mm	3100	3100	3100	3100	3100	3100	3100
16.0 mm	3200	3200	3200	3200	3200	3200	3200
16.5 mm	3300	3300	3300	3300	3300	3300	3300
17.0 mm	3400	3400	3400	3400	3400	3400	3400
17.5 mm	3500	3500	3500	3500	3500	3500	3500
18.0 mm	3600	3600	3600	3600	3600	3600	3600
18.5 mm	3700	3700	3700	3700	3700	3700	3700
19.0 mm	3800	3800	3800	3800	3800	3800	3800
19.5 mm	3900	3900	3900	3900	3900	3900	3900
20.0 mm	4000	4000	4000	4000	4000	4000	4000
20.5 mm	4100	4100	4100	4100	4100	4100	4100
21.0 mm	4200	4200	4200	4200	4200	4200	4200
21.5 mm	4300	4300	4300	4300	4300	4300	4300
22.0 mm	4400	4400	4400	4400	4400	4400	4400
22.5 mm	4500	4500	4500	4500	4500	4500	4500
23.0 mm	4600	4600	4600	4600	4600	4600	4600
23.5 mm	4700	4700	4700	4700	4700	4700	4700
24.0 mm	4800	4800	4800	4800	4800	4800	4800
24.5 mm	4900	4900	4900	4900	4900	4900	4900
25.0 mm	5000	5000	5000	5000	5000	5000	5000
25.5 mm	5100	5100	5100	5100	5100	5100	5100
26.0 mm	5200	5200	5200	5200	5200	5200	5200
26.5 mm	5300	5300	5300	5300	5300	5300	5300
27.0 mm	5400	5400	5400	5400	5400	5400	5400
27.5 mm	5500	5500	5500	5500	5500	5500	5500
28.0 mm	5600	5600	5600	5600	5600	5600	5600
28.5 mm	5700	5700	5700	5700	5700	5700	5700
29.0 mm	5800	5800	5800	5800	5800	5800	5800
29.5 mm	5900	5900	5900	5900	5900	5900	5900
30.0 mm	6000	6000	6000	6000	6000	6000	6000
30.5 mm	6100	6100	6100	6100	6100	6100	6100
31.0 mm	6200	6200	6200	6200	6200	6200	6200
31.5 mm	6300	6300	6300	6300	6300	6300	6300
32.0 mm	6400	6400	6400	6400	6400	6400	6400
32.5 mm	6500	6500	6500	6500	6500	6500	6500
33.0 mm	6600	6600	6600	6600	6600	6600	6600
33.5 mm	6700	6700	6700	6700	6700	6700	6700
34.0 mm	6800	6800	6800	6800	6800	6800	6800
34.5 mm	6900	6900	6900	6900	6900	6900	6900
35.0 mm	7000	7000	7000	7000	7000	7000	7000
35.5 mm	7100	7100	7100	7100	7100	7100	7100
36.0 mm	7200	7200	7200	7200	7200	7200	7200
36.5 mm	7300	7300	7300	7300	7300	7300	7300
37.0 mm	7400	7400	7400	7400	7400	7400	7400
37.5 mm	7500	7500	7500	7500	7500	7500	7500
38.0 mm	7600	7600	7600	7600	7600	7600	7600
38.5 mm	7700	7700	7700	7700	7700	7700	7700
39.0 mm	7800	7800	7800	7800	7800	7800	7800
39.5 mm	7900	7900	7900	7900	7900	7900	7900
40.0 mm	8000	8000	8000	8000	8000	8000	8000
40.5 mm	8100	8100	8100	8100	8100	8100	8100
41.0 mm	8200	8200	8200	8200	8200	8200	8200
41.5 mm	8300	8300	8300	8300	8300	8300	8300
42.0 mm	8400	8400	8400	8400	8400	8400	8400
42.5 mm	8500	8500	8500	8500	8500	8500	8500
43.0 mm	8600	8600	8600	8600	8600	8600	8600
43.5 mm	8700	8700	8700	8700	8700	8700	8700
44.0 mm	8800	8800	8800	8800	8800	8800	8800
44.5 mm	8900	8900	8900	8900	8900	8900	8900
45.0 mm	9000	9000	9000	9000	9000	9000	9000
45.5 mm	9100	9100	9100	9100	9100	9100	9100
46.0 mm	9200	9200	9200	9200	9200	9200	9200
46.5 mm	9300	9300	9300	9300	9300	9300	9300
47.0 mm	9400	9400	9400	9400	9400	9400	9400
47.5 mm	9500	9500	9500	9500	9500	9500	9500
48.0 mm	9600	9600	9600	9600	9600	9600	9600
48.5 mm	9700	9700	9700	9700	9700	9700	9700
49.0 mm	9800	9800	9800	9800	9800	9800	9800
49.5 mm	9900	9900	9900	9900	9900	9900	9900
50.0 mm	10000	10000	10000	10000	10000	10000	10000

The results for the "45 volt" mode appear less startling when one takes into account the variations in power output. In the lower half of the table we show the noise power in units of 10^{-15} watts computed from the relation $P_n = T_n - T_a \frac{P}{P_s}$, using $T = 292^\circ K$, and a bandwidth of 2.5 mc.

Thus the figures for P_n represent the actual noise power coming out of the tube in the two 2.5 mc wide bands located symmetrically about the frequency of oscillation at a distance equal to the i-f for the various conditions listed. Each figure is the sum of the power in the two sidebands, which as we shall see later, are in general not equal. It must be remembered that at the P power points the noise/signal ratio P_n/P will be poorer since the useful power P will be decreased by a factor of 2.

Apart from the 45 volt mode there seems to be a regular trend downward in noise power as the transit angle is increased. Because of the very low power obtained in the 45 volt mode it was not possible to use adequate padding between the oscillator and crystal so results for this mode may be in error due to resonance effects. Also in the 45 volt mode the electrons penetrate close to the reflector and the focusing may be badly upset.

Normally we find that the "high/low ratio" is greater than unity but in the case of the 45 volt mode at 90 mc i-f we find a ratio of only .66. This anomalous behavior was occasionally found in other tubes at both X and X bands and has been reported by H. E. Miller of N.T.L. Knipp's theory predicts these ratios in cases of extremely light loading such as would be found here at the 45 volt mode when the loading was correctly adjusted for the 160 volt mode.

In Table IIa we summarize results obtained for a representative group of 723A/7 tubes, all in the "105 volt" reflector mode and with a 30 mc i-f. Values of $T_n - T_a$ are given for the "head on" condition and at the two half power points, in columns three to five. Column six gives the high/low ratio and seven the power output in milliwatts. Next we have I_0 , the useful current, which makes a second trip through the gap after reflection, which was estimated from the observed cathode current I_k (column 8). In the tenth column we give the electrical tuning range between half power points, and in the last the noise power P_n for the head on condition computed as before.

The tubes reported here were selected to represent the widest variations in overall performance that we could find in our stock, excluding those which were obviously rejects. The estimate of I_0 was formed from observations a) of the cathode and reflector current when the reflector was positive and collecting all electrons which made one trip through the cavity and b) of the cathode current with negative reflector. Ignoring effects of secondaries (which is surely a questionable procedure) we could compute transparencies of the three grids (G_1 and G_2 are similar). These turned out to be in quite good agreement with the optical transparencies, which is our only justification for neglecting the secondaries. With these data the current which was reflected and made a second trip through G_2 could be estimated. Obviously only this current counts for power production, although noise and beam loading can, of course, be contributed by the current which gets past G_2 on its first trip. In many cases operation at positive reflector liberated considerable gas, so all tubes were put through a suitable aging before measurements were made.

We find that although power output varied over a range of almost 2:1 and electrical tuning varied over a range of about 2.5:1, the noise at head on varied about 4:1. So far we have not found any direct correlation between noise output and any of the other quantities recorded.

Table 11a

1-4" x 30 mm. *205 valve" wide

7034/4

Time	RT ₁	$T_{11} - T_0$ °C/m	$T_{11} - T_0$ °C/m	$T_{11} - T_0$ °C/m	Heat Output	$T_{11} - T_0$ °C/m	$T_{11} - T_0$ °C/m	Electrical Heating Index	T_{11}
1000	1.1	1.1	1.1	1.1	1.1	1.1	1.1	1.1	1.1
1100	1.2	1.2	1.2	1.2	1.2	1.2	1.2	1.2	1.2
1200	1.3	1.3	1.3	1.3	1.3	1.3	1.3	1.3	1.3
1300	1.4	1.4	1.4	1.4	1.4	1.4	1.4	1.4	1.4
1400	1.5	1.5	1.5	1.5	1.5	1.5	1.5	1.5	1.5
1500	1.6	1.6	1.6	1.6	1.6	1.6	1.6	1.6	1.6
1600	1.7	1.7	1.7	1.7	1.7	1.7	1.7	1.7	1.7
1700	1.8	1.8	1.8	1.8	1.8	1.8	1.8	1.8	1.8
1800	1.9	1.9	1.9	1.9	1.9	1.9	1.9	1.9	1.9
1900	2.0	2.0	2.0	2.0	2.0	2.0	2.0	2.0	2.0
2000	2.1	2.1	2.1	2.1	2.1	2.1	2.1	2.1	2.1
2100	2.2	2.2	2.2	2.2	2.2	2.2	2.2	2.2	2.2
2200	2.3	2.3	2.3	2.3	2.3	2.3	2.3	2.3	2.3
2300	2.4	2.4	2.4	2.4	2.4	2.4	2.4	2.4	2.4
2400	2.5	2.5	2.5	2.5	2.5	2.5	2.5	2.5	2.5
2500	2.6	2.6	2.6	2.6	2.6	2.6	2.6	2.6	2.6
2600	2.7	2.7	2.7	2.7	2.7	2.7	2.7	2.7	2.7
2700	2.8	2.8	2.8	2.8	2.8	2.8	2.8	2.8	2.8
2800	2.9	2.9	2.9	2.9	2.9	2.9	2.9	2.9	2.9
2900	3.0	3.0	3.0	3.0	3.0	3.0	3.0	3.0	3.0
3000	3.1	3.1	3.1	3.1	3.1	3.1	3.1	3.1	3.1
3100	3.2	3.2	3.2	3.2	3.2	3.2	3.2	3.2	3.2
3200	3.3	3.3	3.3	3.3	3.3	3.3	3.3	3.3	3.3
3300	3.4	3.4	3.4	3.4	3.4	3.4	3.4	3.4	3.4
3400	3.5	3.5	3.5	3.5	3.5	3.5	3.5	3.5	3.5
3500	3.6	3.6	3.6	3.6	3.6	3.6	3.6	3.6	3.6
3600	3.7	3.7	3.7	3.7	3.7	3.7	3.7	3.7	3.7
3700	3.8	3.8	3.8	3.8	3.8	3.8	3.8	3.8	3.8
3800	3.9	3.9	3.9	3.9	3.9	3.9	3.9	3.9	3.9
3900	4.0	4.0	4.0	4.0	4.0	4.0	4.0	4.0	4.0
4000	4.1	4.1	4.1	4.1	4.1	4.1	4.1	4.1	4.1
4100	4.2	4.2	4.2	4.2	4.2	4.2	4.2	4.2	4.2
4200	4.3	4.3	4.3	4.3	4.3	4.3	4.3	4.3	4.3
4300	4.4	4.4	4.4	4.4	4.4	4.4	4.4	4.4	4.4
4400	4.5	4.5	4.5	4.5	4.5	4.5	4.5	4.5	4.5
4500	4.6	4.6	4.6	4.6	4.6	4.6	4.6	4.6	4.6
4600	4.7	4.7	4.7	4.7	4.7	4.7	4.7	4.7	4.7
4700	4.8	4.8	4.8	4.8	4.8	4.8	4.8	4.8	4.8
4800	4.9	4.9	4.9	4.9	4.9	4.9	4.9	4.9	4.9
4900	5.0	5.0	5.0	5.0	5.0	5.0	5.0	5.0	5.0
5000	5.1	5.1	5.1	5.1	5.1	5.1	5.1	5.1	5.1
5100	5.2	5.2	5.2	5.2	5.2	5.2	5.2	5.2	5.2
5200	5.3	5.3	5.3	5.3	5.3	5.3	5.3	5.3	5.3
5300	5.4	5.4	5.4	5.4	5.4	5.4	5.4	5.4	5.4
5400	5.5	5.5	5.5	5.5	5.5	5.5	5.5	5.5	5.5
5500	5.6	5.6	5.6	5.6	5.6	5.6	5.6	5.6	5.6
5600	5.7	5.7	5.7	5.7	5.7	5.7	5.7	5.7	5.7
5700	5.8	5.8	5.8	5.8	5.8	5.8	5.8	5.8	5.8
5800	5.9	5.9	5.9	5.9	5.9	5.9	5.9	5.9	5.9
5900	6.0	6.0	6.0	6.0	6.0	6.0	6.0	6.0	6.0
6000	6.1	6.1	6.1	6.1	6.1	6.1	6.1	6.1	6.1
6100	6.2	6.2	6.2	6.2	6.2	6.2	6.2	6.2	6.2
6200	6.3	6.3	6.3	6.3	6.3	6.3	6.3	6.3	6.3
6300	6.4	6.4	6.4	6.4	6.4	6.4	6.4	6.4	6.4
6400	6.5	6.5	6.5	6.5	6.5	6.5	6.5	6.5	6.5
6500	6.6	6.6	6.6	6.6	6.6	6.6	6.6	6.6	6.6
6600	6.7	6.7	6.7	6.7	6.7	6.7	6.7	6.7	6.7
6700	6.8	6.8	6.8	6.8	6.8	6.8	6.8	6.8	6.8
6800	6.9	6.9	6.9	6.9	6.9	6.9	6.9	6.9	6.9
6900	7.0	7.0	7.0	7.0	7.0	7.0	7.0	7.0	7.0
7000	7.1	7.1	7.1	7.1	7.1	7.1	7.1	7.1	7.1
7100	7.2	7.2	7.2	7.2	7.2	7.2	7.2	7.2	7.2
7200	7.3	7.3	7.3	7.3	7.3	7.3	7.3	7.3	7.3
7300	7.4	7.4	7.4	7.4	7.4	7.4	7.4	7.4	7.4
7400	7.5	7.5	7.5	7.5	7.5	7.5	7.5	7.5	7.5
7500	7.6	7.6	7.6	7.6	7.6	7.6	7.6	7.6	7.6
7600	7.7	7.7	7.7	7.7	7.7	7.7	7.7	7.7	7.7
7700	7.8	7.8	7.8	7.8	7.8	7.8	7.8	7.8	7.8
7800	7.9	7.9	7.9	7.9	7.9	7.9	7.9	7.9	7.9
7900	8.0	8.0	8.0	8.0	8.0	8.0	8.0	8.0	8.0
8000	8.1	8.1	8.1	8.1	8.1	8.1	8.1	8.1	8.1
8100	8.2	8.2	8.2	8.2	8.2	8.2	8.2	8.2	8.2
8200	8.3	8.3	8.3	8.3	8.3	8.3	8.3	8.3	8.3
8300	8.4	8.4	8.4	8.4	8.4	8.4	8.4	8.4	8.4
8400	8.5	8.5	8.5	8.5	8.5	8.5	8.5	8.5	8.5
8500	8.6	8.6	8.6	8.6	8.6	8.6	8.6	8.6	8.6
8600	8.7	8.7	8.7	8.7	8.7	8.7	8.7	8.7	8.7
8700	8.8	8.8	8.8	8.8	8.8	8.8	8.8	8.8	8.8
8800	8.9	8.9	8.9	8.9	8.9	8.9	8.9	8.9	8.9
8900	9.0	9.0	9.0	9.0	9.0	9.0	9.0	9.0	9.0
9000	9.1	9.1	9.1	9.1	9.1	9.1	9.1	9.1	9.1
9100	9.2	9.2	9.2	9.2	9.2	9.2	9.2	9.2	9.2
9200	9.3	9.3	9.3	9.3	9.3	9.3	9.3	9.3	9.3
9300	9.4	9.4	9.4	9.4	9.4	9.4	9.4	9.4	9.4
9400	9.5	9.5	9.5	9.5	9.5	9.5	9.5	9.5	9.5
9500	9.6	9.6	9.6	9.6	9.6	9.6	9.6	9.6	9.6
9600	9.7	9.7	9.7	9.7	9.7	9.7	9.7	9.7	9.7
9700	9.8	9.8	9.8	9.8	9.8	9.8	9.8	9.8	9.8
9800	9.9	9.9	9.9	9.9	9.9	9.9	9.9	9.9	9.9
9900	10.0	10.0	10.0	10.0	10.0	10.0	10.0	10.0	10.0
Average		2.79	9.29	9.29	11.06	11.06	11.06	11.06	11.06

In Table IIb we give similar data (omitting the current measurements) for some K-band tubes, mostly 2K32's with a couple of 6022A's shown for comparison although they are now obsolete. These were measured with 30 mc i-f and in a reflector voltage mode occurring near 200 volts. It is not at all certain that we were using the same drift angle in all cases. In this case the crystal had a conversion loss of 8.2 db and a noise temperature of 2.

As is only to be expected, the noise is increased since the ratio of i-f to r-f is smaller and a large increase in Q of the oscillator is very unlikely. If we compute the noise to signal ratio, P_n/P , for the case of 3.5 mc bandwidth at 30 mc i-f (two sidebands) we find an average of 5.1×10^{-10} at K band contrasted with 2.33×10^{-10} at X. Considering only the ratio of i-f to r-f in the two cases one would expect a larger difference. The implication is that the loaded Q of the 2K32 tube is somewhat higher than that of the 723A/B, and this is borne out to some extent by the fact that the electrical tuning range is only slightly greater at K-band. In any event there is no real basis for the general impression that K-band tubes are "noisy".

It should be pointed out that in cases where marked electrical tuning hysteresis was present the noise was greatly increased. This may well be due to a combination of effects such as heavy reactive loads and multiple transits. Because of the great difficulties due to instability no quantitative work in the hysteresis region was attempted.

Measurements made on a 723A/B with a rejection filter to eliminate one sideband are presented in Figs. 3 and 4 for 30 and 60 mc i-f respectively. The filter used was of course not perfect and an empirical correction was used to allow for the "leakage" that got past it. The validity of this procedure is shown by the fact that the measured curve for both sidebands agree quite well with the sum of the two separated sidebands. Points were taken with the electrical tuning "hand on" and detuned to the 3/4, 1/2 and 1/4 power points on each side. Note that at hand on, the two sidebands are by no means symmetrical. This at first made us think we had chosen the center of the mode incorrectly, until we learned that Knipp predicted just this effect.

The vertical broken lines represent the limits of oscillation. We were unable to make good measurements much below the 1/4 power points, so we have sketched in the rest of the curves as predicted by Knipp's theory. We see now that the high-low ratio is principally due to the behavior of the low frequency sideband.

The effect of load variations on the noise output of a 723A/B is shown in Fig. 5, which is an admittance plot with the plane of reference at the grids of the tubes. This was taken at 30 mc i-f, and the sidebands were not separated. The reflector voltage was set at the center of the mode at matched load. The numbers give noise power in arbitrary units. As might be expected the noise is least for light loads and increases to very high values near the sink.

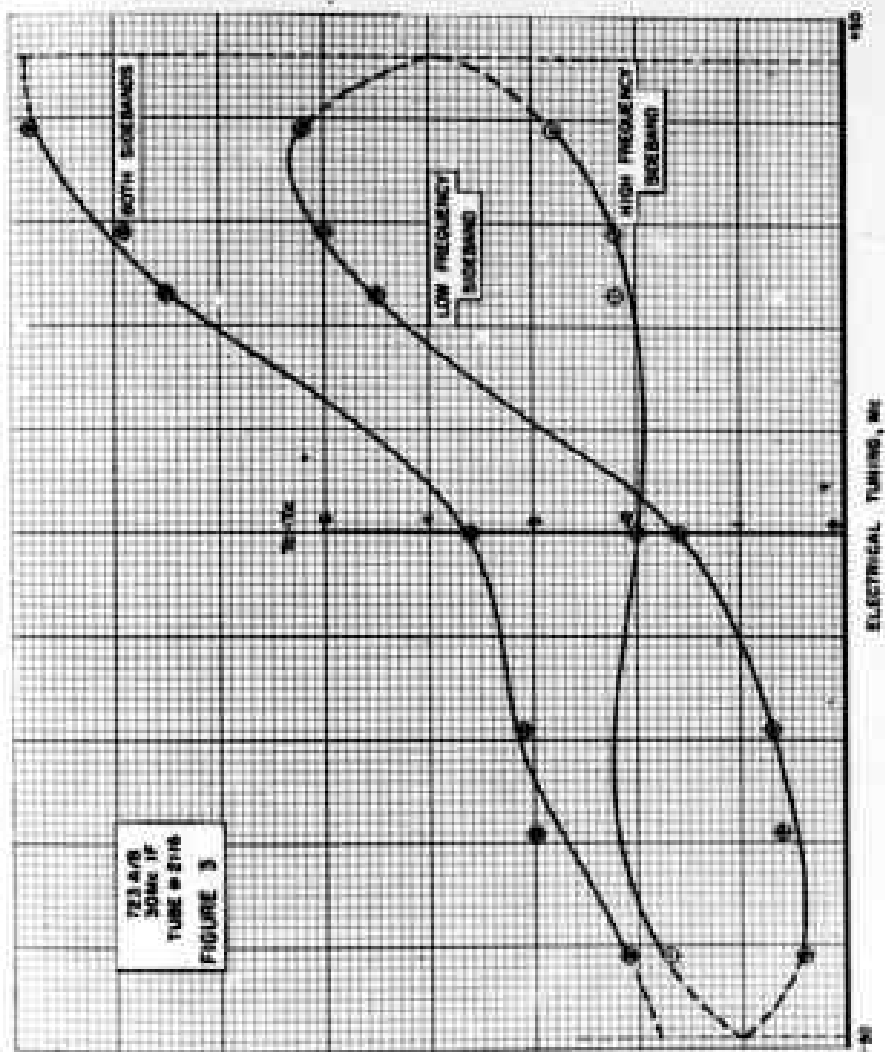
Note that the noise contours do not follow the conductance lines exactly, but that the tube is more noisy for inductive loads. This is a consequence of the long line effect plus the fact that the two sidebands contain different amounts of noise power. For each point on the diagram representing a particular load admittance we observed the power due to two sidebands. Because the load was not really at the grids but was actually several wavelengths away, the loads seen by the two sidebands 30 mc above and below the center frequency were appreciably different. Taking this effect into account and using Knipp's curves for the power in the two sidebands as a function

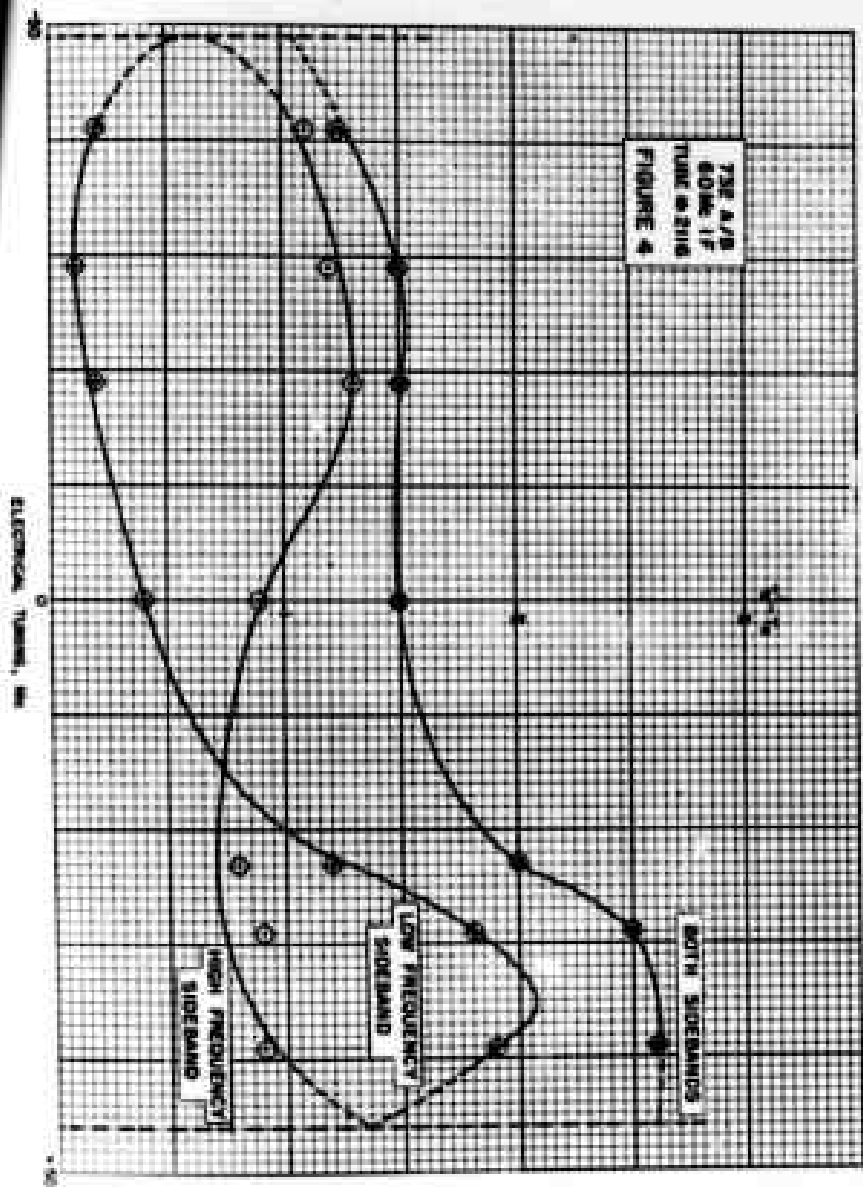
5. For a discussion of the method of representation see RL Report No. 717, Notes on Load Effects on Reflector Oscillators

Table 12b

1-2 = 30 sec *500 watts mode

Time	Type	$T_b' - T_a$ heat sec.	$T_p' - T_a$ $\frac{1}{2}$ sec.	$T_p' - T_a$ $\frac{1}{2}$ min.	M/1a	Power Output	Electrical Thrilling Range	P_b
20	2033	1.0	9.0	13.1	1.6	35.4 sec	25 sec	1.7×10^{-12} w
25	"	1.2	7.7	12.7	1.7	35.2	25	151
30	"	1.4	6.4	12.0	1.7	35.0	25	151
35	"	1.6	5.6	11.3	1.7	34.8	25	151
40	"	1.8	4.8	10.6	1.7	34.6	25	151
45	"	2.0	4.0	10.0	1.7	34.4	25	151
50	"	2.2	3.2	9.3	1.7	34.2	25	151
55	"	2.4	2.4	8.6	1.7	34.0	25	151
60	"	2.6	1.6	7.9	1.7	33.8	25	151
65	"	2.8	0.8	7.2	1.7	33.6	25	151
70	"	3.0	0.0	6.5	1.7	33.4	25	151
75	"	3.2	-0.8	5.8	1.7	33.2	25	151
80	"	3.4	-1.6	5.1	1.7	33.0	25	151
85	"	3.6	-2.4	4.4	1.7	32.8	25	151
90	"	3.8	-3.2	3.7	1.7	32.6	25	151
95	"	4.0	-4.0	3.0	1.7	32.4	25	151
100	"	4.2	-4.8	2.3	1.7	32.2	25	151
105	"	4.4	-5.6	1.6	1.7	32.0	25	151
110	"	4.6	-6.4	0.9	1.7	31.8	25	151
115	"	4.8	-7.2	0.2	1.7	31.6	25	151
120	"	5.0	-8.0	-0.5	1.7	31.4	25	151
125	"	5.2	-8.8	-1.2	1.7	31.2	25	151
130	"	5.4	-9.6	-1.9	1.7	31.0	25	151
135	"	5.6	-10.4	-2.6	1.7	30.8	25	151
140	"	5.8	-11.2	-3.3	1.7	30.6	25	151
145	"	6.0	-12.0	-4.0	1.7	30.4	25	151
150	"	6.2	-12.8	-4.7	1.7	30.2	25	151
155	"	6.4	-13.6	-5.4	1.7	30.0	25	151
160	"	6.6	-14.4	-6.1	1.7	29.8	25	151
165	"	6.8	-15.2	-6.8	1.7	29.6	25	151
170	"	7.0	-16.0	-7.5	1.7	29.4	25	151
175	"	7.2	-16.8	-8.2	1.7	29.2	25	151
180	"	7.4	-17.6	-8.9	1.7	29.0	25	151
185	"	7.6	-18.4	-9.6	1.7	28.8	25	151
190	"	7.8	-19.2	-10.3	1.7	28.6	25	151
195	"	8.0	-20.0	-11.0	1.7	28.4	25	151
200	"	8.2	-20.8	-11.7	1.7	28.2	25	151
205	"	8.4	-21.6	-12.4	1.7	28.0	25	151
210	"	8.6	-22.4	-13.1	1.7	27.8	25	151
215	"	8.8	-23.2	-13.8	1.7	27.6	25	151
220	"	9.0	-24.0	-14.5	1.7	27.4	25	151
225	"	9.2	-24.8	-15.2	1.7	27.2	25	151
230	"	9.4	-25.6	-15.9	1.7	27.0	25	151
235	"	9.6	-26.4	-16.6	1.7	26.8	25	151
240	"	9.8	-27.2	-17.3	1.7	26.6	25	151
245	"	10.0	-28.0	-18.0	1.7	26.4	25	151
250	"	10.2	-28.8	-18.7	1.7	26.2	25	151
255	"	10.4	-29.6	-19.4	1.7	26.0	25	151
260	"	10.6	-30.4	-20.1	1.7	25.8	25	151
265	"	10.8	-31.2	-20.8	1.7	25.6	25	151
270	"	11.0	-32.0	-21.5	1.7	25.4	25	151
275	"	11.2	-32.8	-22.2	1.7	25.2	25	151
280	"	11.4	-33.6	-22.9	1.7	25.0	25	151
285	"	11.6	-34.4	-23.6	1.7	24.8	25	151
290	"	11.8	-35.2	-24.3	1.7	24.6	25	151
295	"	12.0	-36.0	-25.0	1.7	24.4	25	151
300	"	12.2	-36.8	-25.7	1.7	24.2	25	151
305	"	12.4	-37.6	-26.4	1.7	24.0	25	151
310	"	12.6	-38.4	-27.1	1.7	23.8	25	151
315	"	12.8	-39.2	-27.8	1.7	23.6	25	151
320	"	13.0	-40.0	-28.5	1.7	23.4	25	151
325	"	13.2	-40.8	-29.2	1.7	23.2	25	151
330	"	13.4	-41.6	-29.9	1.7	23.0	25	151
335	"	13.6	-42.4	-30.6	1.7	22.8	25	151
340	"	13.8	-43.2	-31.3	1.7	22.6	25	151
345	"	14.0	-44.0	-32.0	1.7	22.4	25	151
350	"	14.2	-44.8	-32.7	1.7	22.2	25	151
355	"	14.4	-45.6	-33.4	1.7	22.0	25	151
360	"	14.6	-46.4	-34.1	1.7	21.8	25	151
365	"	14.8	-47.2	-34.8	1.7	21.6	25	151
370	"	15.0	-48.0	-35.5	1.7	21.4	25	151
375	"	15.2	-48.8	-36.2	1.7	21.2	25	151
380	"	15.4	-49.6	-36.9	1.7	21.0	25	151
385	"	15.6	-50.4	-37.6	1.7	20.8	25	151
390	"	15.8	-51.2	-38.3	1.7	20.6	25	151
395	"	16.0	-52.0	-39.0	1.7	20.4	25	151
400	"	16.2	-52.8	-39.7	1.7	20.2	25	151
405	"	16.4	-53.6	-40.4	1.7	20.0	25	151
410	"	16.6	-54.4	-41.1	1.7	19.8	25	151
415	"	16.8	-55.2	-41.8	1.7	19.6	25	151
420	"	17.0	-56.0	-42.5	1.7	19.4	25	151
425	"	17.2	-56.8	-43.2	1.7	19.2	25	151
430	"	17.4	-57.6	-43.9	1.7	19.0	25	151
435	"	17.6	-58.4	-44.6	1.7	18.8	25	151
440	"	17.8	-59.2	-45.3	1.7	18.6	25	151
445	"	18.0	-60.0	-46.0	1.7	18.4	25	151
450	"	18.2	-60.8	-46.7	1.7	18.2	25	151
455	"	18.4	-61.6	-47.4	1.7	18.0	25	151
460	"	18.6	-62.4	-48.1	1.7	17.8	25	151
465	"	18.8	-63.2	-48.8	1.7	17.6	25	151
470	"	19.0	-64.0	-49.5	1.7	17.4	25	151
475	"	19.2	-64.8	-50.2	1.7	17.2	25	151
480	"	19.4	-65.6	-50.9	1.7	17.0	25	151
485	"	19.6	-66.4	-51.6	1.7	16.8	25	151
490	"	19.8	-67.2	-52.3	1.7	16.6	25	151
495	"	20.0	-68.0	-53.0	1.7	16.4	25	151
500	"	20.2	-68.8	-53.7	1.7	16.2	25	151
505	"	20.4	-69.6	-54.4	1.7	16.0	25	151
510	"	20.6	-70.4	-55.1	1.7	15.8	25	151
515	"	20.8	-71.2	-55.8	1.7	15.6	25	151
520	"	21.0	-72.0	-56.5	1.7	15.4	25	151
525	"	21.2	-72.8	-57.2	1.7	15.2	25	151
530	"	21.4	-73.6	-57.9	1.7	15.0	25	151
535	"	21.6	-74.4	-58.6	1.7	14.8	25	151
540	"	21.8	-75.2	-59.3	1.7	14.6	25	151
545	"	22.0	-76.0	-60.0	1.7	14.4	25	151
550	"	22.2	-76.8	-60.7	1.7	14.2	25	151
555	"	22.4	-77.6	-61.4	1.7	14.0	25	151
560	"	22.6	-78.4	-62.1	1.7	13.8	25	151
565	"	22.8	-79.2	-62.8	1.7	13.6	25	151
570	"	23.0	-80.0	-63.5	1.7	13.4	25	151
575	"	23.2	-80.8	-64.2	1.7	13.2	25	151
580	"	23.4	-81.6	-64.9	1.7	13.0	25	151
585	"	23.6	-82.4	-65.6	1.7	12.8	25	151
590	"	23.8	-83.2	-66.3	1.7	12.6	25	151
595	"	24.0	-84.0	-67.0	1.7	12.4	25	151
600	"	24.2	-84.8	-67.7	1.7	12.2	25	151
605	"	24.4	-85.6	-68.4	1.7	12.0	25	151
610	"	24.6	-86.4	-69.1	1.7	11.8	25	151
615	"	24.8	-87.2	-69.8	1.7	11.6	25	151
620	"	25.0	-88.0	-70.5	1.7	11.4	25	151
625	"	25.2	-88.8	-71.2	1.7	11.2	25	151
630	"	25.4	-89.6	-71.9	1.7	11.0	25	151
635	"	25.6	-90.4	-72.6	1.7	10.8	25	151
640	"	25.8	-91.2	-73.3	1.7	10.6	25	151
645	"	26.0	-92.0	-74.0	1.7	10.4	25	151
650	"	26.2	-92.8	-74.7	1.7	10.2	25	151
655	"	26.4	-93.6	-75.4	1.7	10.0	25	151
660	"	26.6	-94.4	-76.1	1.7	9.8	25	151
665	"	26.8	-95.2	-76.8	1.7	9.6	25	151
670	"	27.0	-96.0	-77.5	1.7	9.4	25	151
675	"	27.2	-96.8	-78.2	1.7	9.2	25	151
680	"	27.4	-97.6	-78.9	1.7	9.0	25	151
685	"	27.6	-98.4	-79.6	1.7	8.8	25	151
690	"	27.8	-99.2	-80.3	1.7	8.6	25	151
695	"	28.0	-100.0	-81.0	1.7	8.4	25	151
700	"	28.2	-100.8	-81.7	1.7	8.2	25	151
705	"	28.4	-101.6	-82.4	1.7	8.0	25	151
710	"	28.6	-102.4	-83.1	1.7	7.8	25	151
715	"	28.8	-103.2	-83.8	1.7	7.6	25	151
720	"	29.0	-104.0	-84.5	1.7	7.4	25	151
725	"	29.2	-104.8	-85.2	1.7	7.2	25	151
730	"	29.4	-105.6	-85.9	1.7	7.0	25	151
735	"	29.6	-106.4	-86.6	1.7	6.8	25	151
740	"	29.8	-107.2	-87.3	1.7	6.6	25	151
745	"	30.0	-108.0	-88.0	1.7	6.4	25	151
750	"	30.2	-108.8	-88.7	1.7	6.2	25	151
755	"	30.4	-109.6	-89.4	1.7	6.0	25	151
760	"	30.6	-110.4	-90.1	1.7	5.8	25	151
765	"	30.8	-111.2	-90.8	1.7	5.6	25	151
770	"	31.0	-112.0	-91.5	1.7	5.4	25	151
775	"	31.2	-112.8	-92.2	1.7	5.2	25	151
780	"	31.4	-113.6	-92.9	1.7	5.0	25	151
785	"	31.6	-114.4	-93.6	1.7	4.8	25	151
790	"	31.8	-115.2	-94.3	1.7	4.6	25	151
795	"	32.0	-116.0	-95.0	1.7	4.4	25	151
800	"	32.2	-116.8	-95.7	1.7	4.2	25	151</





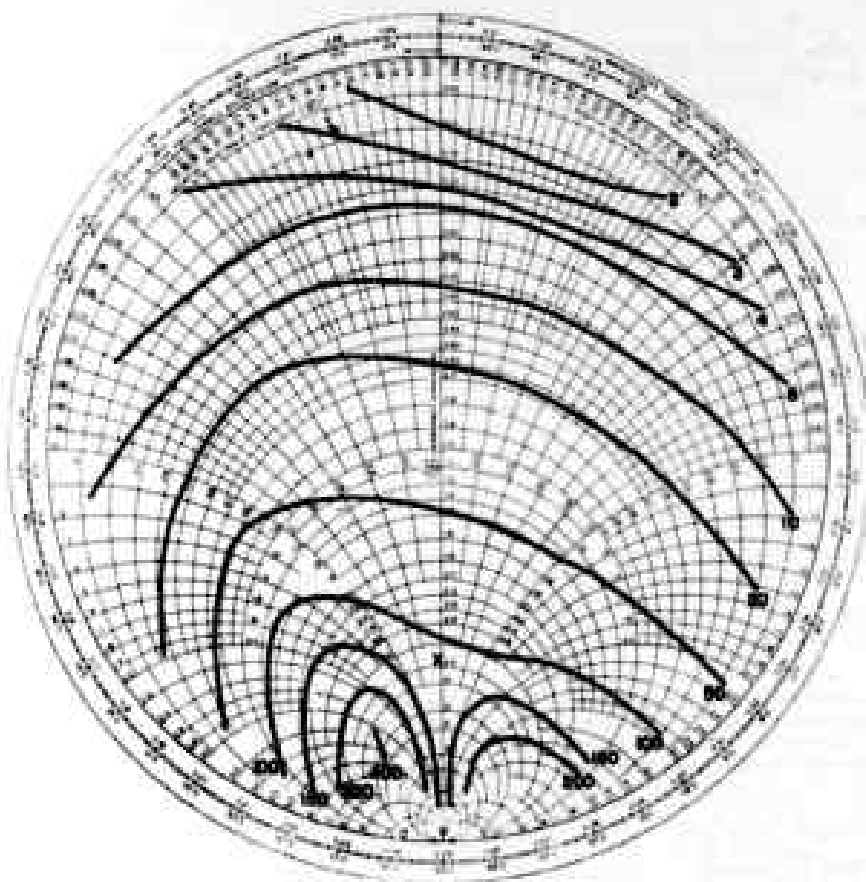


FIGURE 5 NOISE OUTPUT OF A 723 A/B AS A FUNCTION OF LOAD ADMITTANCE. I.F. 30MC, BOTH SIDEBANDS. NUMBERS ARE % MAX POWER $X(T_C' - T_C)$ WHERE $(T_C' - T_C)$ ARE IN TEMP. UNITS. THE CROSS INDICATES THE MAXIMUM POWER POINT.

of load conductance we could compute the theoretical diagram shown in Fig. 8. This is drawn for a hypothetical tube. The scale again is in arbitrary units. Note the strong resemblance in the shape of the contours to those found experimentally.

Discussion

The rather high values shown in Tables I and II under P_n , ranging upward of 10^{-11} watts, should not cause undue alarm since it must be remembered that in operating receivers there will be several factors reducing the amount of this noise reaching the receiver input. In the first place, the decoupling used to adjust the excitation for the mixer will operate on the noise sidebands also, and ordinarily to the same extent.

Second, many converters have a tuned circuit in the input (e.g. a tunable TR box) which profoundly affects results. If the Q is sufficiently high, and the box is tuned for signals, local oscillator frequency and image frequency will be reflected well. If the phase of the reflected local oscillator voltage is right to add to the direct wave at the crystal it will be possible to decouple by 6 db more than if local oscillator is fed in through a matched line as in these experiments. At the same time one noise sideband (that at image frequency) will be similarly reinforced. The sideband at signal frequency will be transmitted through the TR, leaving only the direct wave, so there will be a net reduction in noise power converted. The amount of this improvement can readily be computed for any specific case. The results depend strongly on the parameters chosen, but reductions of 25 to 50% are common. It is perhaps interesting to note that the common practice of putting the local oscillator on the high frequency side of the signal (so that the low frequency sideband is reduced) tends to minimize the increase in noise figure with electrical tuning. With this arrangement the noise figure would be slightly poorer at the center of the mode but would not decay nearly as fast when electrical tuning toward higher frequencies is required.

Third, the load seen by the oscillator itself may not be as heavy as we used. Oscillators are often underloaded for the sake of securing more uniform output over a wide tuning range. From Fig. 5 we see that comparatively small changes in load which would not materially affect the power output may make considerable differences in the noise.

J. B. H. Kuper
M. C. Walte
October 30, 1945

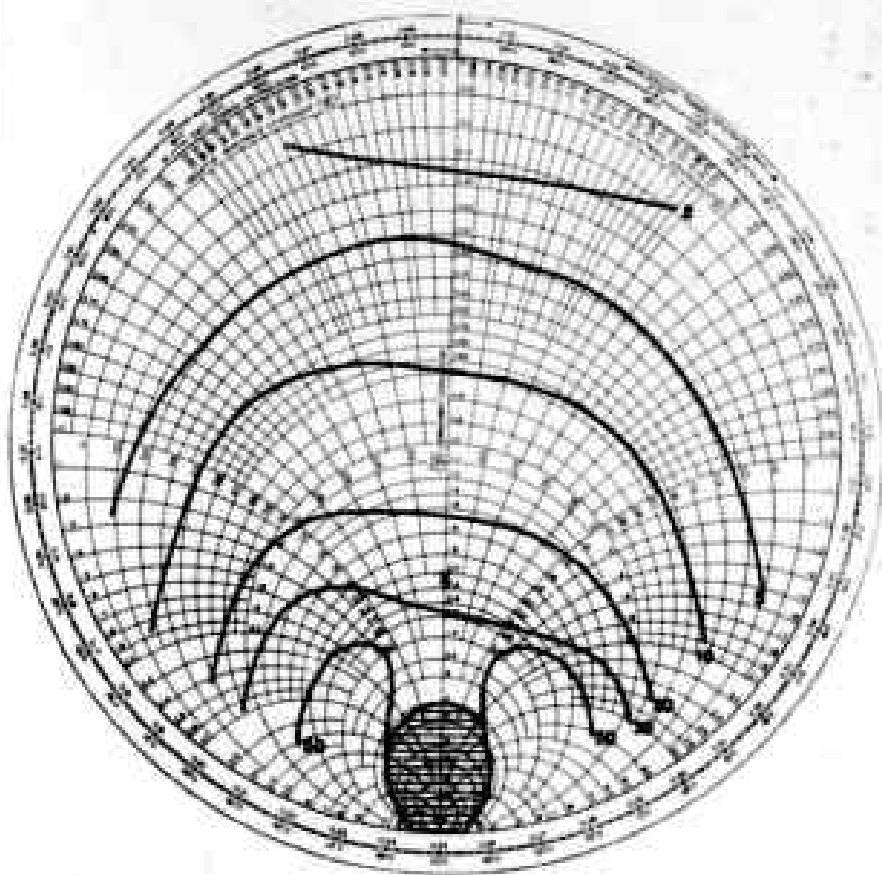


FIGURE 6 NOISE CONTOURS FOR 30MC IF, HYPOTHETICAL TUBE LINE 3A LONG. UNITS ARE $10 \times F \times g$, WHERE F IS FROM KNIPP'S REPORT, AND g IS CONDUCTANCE AT GRIDS NORMALIZED TO ONE AT SINK. THE CROSS INDICATES MAXIMUM POWER POINT.

REEL - C

4 8 2

A.T.I.

1 3 8 0 0

CADO CONTROL NO:

U S CLASSIFICATION:

ATI NO:

CA NO:

Unclase.

ATX 13800

REC-72

TITLE:

Measurements on Noise from Reflex Oscillators

AUTHOR(S):

Kuper, J.B.H.

ORIGINATING AGENCY:

Mass. Inst. of Technology, Radiation Lab., Cambridge

FOREIGN TITLES:

PUBLISHED BY:

OSRD, IDRC, Div 11

PUBLISHING NO:

None

TRANSLATED BY:

TRANSLATION NO:

PREVIOUSLY CATALOGED AS:

WP-1-10 AUG 68 450M

THE UNIVERSITY OF CHICAGO

(23) * Reflex Klystrons;
TITLE: Measurements on Noise from Reflex Oscillators

AUTHOR(S): Kuper, J. B. H.

ORIGINATING AGENCY: Massachusetts Inst. of Technology, Radiation Lab., Cambridge

PUBLISHED BY: Office of Scientific Research and Development, Div. 14, Washington, D. C.

ATI- 24494 (25)

REVISION (None)

ORIG. AGENCY NO.
R-872

PUBLISHING AGENCY NO.
(None)

DATE
Oct '45

DOC. CLASS.
Unclass.

COUNTRY
U.S.

LANGUAGE
Eng.

PAGES
16

ILLUSTRATIONS
tables, diagrs, graphs

ABSTRACT:

A program of measurements on noise output of reflex local oscillators, particularly the 723A/B and 2K33, was undertaken to determine the importance of this factor in receiver design. Considering the two noise sidebands each 2.5 mcps wide and located 30 mcps away from the main output, noise powers ranging from 2.2 to 9.8×10^{-12} watts coming out of 723A/B's were found when loaded for optimum output. Asymmetrical behavior of the noise with electronic tuning was investigated and found to require the new theory presented in the report to follow. Some measurements of the individual noise sidebands and of the noise output as a function of load were found to be in satisfactory agreement with theory.

DISTRIBUTION: Copies of this report obtainable from Air Documents Division; Attn: MCDXD

DIVISION: Electronics (2)

SECTION: Static and interferences (4)

SUBJECT HEADINGS: Oscillators, Reflex - Noise (68492.325)

ATI SHEET NO.: R-3-4-18

Air Documents Division, Intelligence Department
Air Materiel Command

AIR TECHNICAL INDEX

Wright-Patterson Air Force Base
Dayton, Ohio